1-30-2018

Lanthanum-Mediated Dehydrogenation of Butenes: Spectroscopy and Formation of $La(C_4H_6)$ Isomers

Wenjin Cao
University of Kentucky, wj.cao0707@uky.edu

Dilkrushi Hewage
University of Kentucky, dche223@uky.edu

Dong-Sheng Yang
University of Kentucky, Dong-Sheng.Yang@uky.edu

Lanthanum-mediated dehydrogenation of butenes: Spectroscopy and formation of La(C_4H_6) isomers

Wenjin Cao, Dilrukshi Hewage, and Dong-Sheng Yang

Citation: J. Chem. Phys. **148**, 044312 (2018); doi: 10.1063/1.5017615
View online: https://doi.org/10.1063/1.5017615
View Table of Contents: http://aip.scitation.org/toc/jcp/148/4
Published by the American Institute of Physics

Lanthanum-mediated dehydrogenation of butenes: Spectroscopy and formation of La(C_4H_6) isomers

Wenjin Cao, Dilrukshi Hewage, and Dong-Sheng Yang[a)]
Department of Chemistry, University of Kentucky, Lexington, Kentucky 40506-0055, USA

(Received 28 November 2017; accepted 16 January 2018; published online 30 January 2018)

La atom reactions with 1-butene, 2-butene, and isobutene are carried out in a laser-vaporization molecular beam source. The three reactions yield the same La-hydrocarbon products from the dehydrogenation and carbon-carbon bond cleavage and coupling of the butenes. The dehydrogenated species La(C_4H_6) is the major product, which is characterized with mass-analyzed threshold ionization (MATI) spectroscopy and quantum chemical computations. The MATI spectrum of La(C_4H_6) produced from the La+1-butene reaction exhibits two band systems, whereas the MATI spectra produced from the La+2-butene and isobutene reactions display only a single band system. Each of these spectra shows a strong origin band and several vibrational progressions. The two band systems from the spectrum of the 1-butene reaction are assigned to the ionization of two isomers: La[$C(CH_2)_3$] (Iso A) and La($CH_2CHCHCH_2$) (Iso B), and the single band system from the spectra of the 2-butene and isobutene reactions is attributed to Iso B and Iso A, respectively. The ground electronic states are $^2A_1$ (C_{3v}) for Iso A and $^2A'$ (C_s) for Iso B. The ionization of the doublet state of each isomer removes a La 6s-based electron and leads to the $^1A_1$ ion of Iso A and the $^1A'$ ion of Iso B. The formation of both isomers consists of La addition to the C=C double bond, La insertion into two C(sp^3)—H bonds, and H_2 elimination. In addition to these steps, the formation of Iso A from the La+1-butene reaction may involve the isomerization of 1-butene to isobutene prior to the C—H bond activation, whereas the formation of Iso B from the La+*trans*-2-butene reaction may include the *trans*- to *cis*-butene isomerization after the C—H bond activation. *Published by AIP Publishing.*
https://doi.org/10.1063/1.5017615

I. INTRODUCTION

Spectroscopy of transition metal-hydrocarbon radicals or ions formed in gas phase reactions has recently attracted considerable attention. Metal ion-hydrocarbon species are largely investigated by infrared or ultraviolet-visible photodissociation or photoelectron spectroscopy,[1–20] whereas metal atom-hydrocarbon radicals are mainly studied by resonant two-photon ionization and dispersed fluorescence,[21–24] Fourier transform microwave,[25] and mass-analyzed threshold ionization (MATI) spectroscopy.[26–33] Spectroscopic measurements probe the state specific energetics and structures of short-lived species, which are vital for gaining insight into reaction mechanisms and electronic and structural characteristics for efficient bond activation at metal centers. Such measurements can also be used to validate electronic structure calculations, where the computations are complicated by possibly multiple low-energy isomers of each metal-containing species and high-dense low-lying electronic states or spin-orbit levels of each isomer. On the other hand, spectroscopic measurements of transition metal-hydrocarbon radicals formed by the C—H or C—C bond activation of hydrocarbon compounds encounter substantial challenges because such radicals are produced with low number density. We have recently reported the MATI spectroscopy and formation of the metal-hydrocarbon radicals produced by the lanthanide-mediated C—C and C—H bond activation of several small alkenes and alkynes.[26–33] Our studies have demonstrated that the combination of the MATI spectroscopic measurements with theoretical computations is a powerful approach to investigate transient metal-hydrocarbon species.

Butene (C_4H_6) has three common structural isomers: 1-butene (CH_2=$CHCH_2CH_3$), 2-butene (CH_3CH=$CHCH_3$), and 2-methylpropene or isobutene (CH_2=$C(CH_3)_2$). Their reactions with metal ions have been investigated with mass-spectrometry-based techniques.[34–45] For 1- and 2-butenes, loss of H_2 is the exclusive or predominate reaction with M^+ = Sc^+, Fe^+, Co^+, Ni^+, Ln^+, and Pt^+; Ln = lanthanide and leads to presumably butadiene complexes $M^+(C_4H_6)$.[34,36,38,39,41,44] This contrasts the behavior of isobutene, which formed only sequential adducts with Fe^+ but is dehydrogenated by Co^+, Ni^+, and Sc^+ to form $M^+(C_4H_6)$.[38,39] Collision-induced dissociation, ion-molecule reactions, and deuterium exchanges indicated that the $M^+(C_4H_6)$ ions generated from the isobutene reactions were likely M^+(butadiene) with M^+ = Co^+ or Ni^+[38] but M^+(trimethylenemethane) with M^+ = Sc^+.[39] Dehydrogenation of the butenes has also been observed by various transition metal atoms.[35,46–49] For example, Y(C_4H_6)+H_2 was observed using crossed molecular beams as the predominant process for the Y reactions with 1-butene, 2-butene, and isobutene at collision energies of 11.0 and 26.6 kcal mol^{-1},

a)Author to whom correspondence should be addressed: dyang0@uky.edu

although $Y(H_2)+C_4H_6$ was also detected as a significant channel for Y+1- and 2-butenes at the 26.6 kcal mol^{-1} collision energy.[49]

In this article, we report the spectroscopic characterization of $La(C_4H_6)$ formed by La reactions with the three isomers of the butenes using MATI spectroscopy. The motivation was to determine spectroscopically the structures of the dehydrogenated species and to understand how a La atom activates the C—H bonds and removes H_2 from the butenes. To our knowledge, this is the first vibronic spectroscopic measurement of metal radicals formed by the C—H bond activation of the butenes.

II. EXPERIMENTAL AND COMPUTATIONAL METHODS

A. Experimental

The metal-cluster beam instrument used in this work consists of reaction and spectroscopy vacuum chambers and was described in a previous publication.[50] Metal-hydrocarbon reactions were carried out in a laser-ablation metal cluster beam source. Each of the gaseous butenes (1-butene, 2-butene, and isobutene: ≥99%, Aldrich) was seeded in a He (99.998%, Scott Gross) carrier gas with a butene: He molar ratio of $\sim 10^{-5}$-10^{-7} in a stainless steel mixing cylinder. La atoms were generated by pulsed-laser (Nd:YAG, Continuum Minilite II, 532 nm, ~1.0 mJ/pulse) ablation of a La rod (99.9%, Alfa Aesar) in the presence of the butene/carrier gas mixture (40 psi) delivered by a home-made piezoelectric pulsed valve. The metal atoms and gas mixture entered into a collision tube (2 mm diameter and 2 cm length), were then expanded into the reaction chamber, collimated by a cone-shaped skimmer (2 mm inner diameter), and passed through a pair of deflection plates. Ionic species in the molecular beam that was formed by laser ablation were removed by an electric field (100 V cm^{-1}) applied on the deflection plates, and neutral products were identified by photoionization TOF mass spectrometry.

Prior to the MATI measurements, photoionization efficiency spectra of $La(C_4H_6)$ were recorded to locate an approximate ionization threshold to guide MATI scans. In the MATI experiment, $La(C_4H_6)$ was excited to high-lying Rydberg states in a single-photon process and ionized by a delayed pulsed electric field. The excitation laser was the frequency doubled output of a tunable dye laser (Lumonics HD-500), pumped by the third harmonic output (355 nm) of a Nd:YAG laser (Continuum Surelite II). The laser beam was collinear and counter propagating with the molecular beam. The ionization pulsed field (320 V cm^{-1}), which was also used for accelerating ions into the field free region, was generated by two high voltage pulse generators (DEI, PVX-4140) and delayed by ~20 μs from the laser pulse by a delayed pulsed generator (SRS, DG645). A small dc field (6.0 V cm^{-1}) from another power supply (GW INSTEK, GPS-30300) was used to separate the ions produced by direct photoionization from the MATI ions generated by the delayed field ionization. The MATI ion signal was obtained by scanning the tunable dye laser, detected by a dual microchannel plate detector, amplified by a preamplifier (SRS, SR445), visualized by a digital oscilloscope (Tektronix TDS 3012), and stored in a laboratory computer. Laser wavelengths were calibrated against titanium atomic transitions in the MATI spectral region, and the calibration was done after recording the MATI spectra.[51] The Stark shift on the adiabatic ionization energy (ΔAIE) induced by the dc field (E_f) was calculated using the relation of $\Delta AIE = 6.1E_f^{1/2}$, where E_f is in V cm^{-1} and ΔAIE is in cm^{-1}.[52]

B. Computational

Density functional theory (DFT) method with the Becke's three-parameter hybrid functional with the correlation functional of Lee, Yang, and Parr (B3LYP) was used to calculate the equilibrium geometries and vibrational frequencies of various isomers of $La(C_4H_6)$ and the free ligands. The basis sets used in these calculations were 6-311+G(d,p) for C and H and the Stuttgart/Dresden (SDD) effective-core-potential basis set with 28 electron core for La. We have extensively used the DFT/B3LYP method and found that this method generally produced adequate results for spectral and structural assignments of organometallic radicals.[26–28,30–32,53] No symmetry restrictions were imposed in initial geometry optimizations, but appropriate point groups were used in subsequent optimizations to help identify electronic symmetries. For each optimized stationary point, a vibrational analysis was performed to identify the nature of the stationary point (minimum or saddle point). In predicting reaction pathways, minima connected by a transition state were confirmed by intrinsic reaction coordinate calculations. To refine the energies of the lowest doublet and singlet states, single-point energy calculations were carried out with the coupled cluster with single, double, and perturbative triple [CCSD(T)] excitations method. These calculations involve the third-order Douglas-Kroll-Hess scalar relativistic correction and at the DFT/B3LYP optimized geometries. Basis sets used in the CCSD(T) calculations were aug-cc-pVTZ-DK[54,55] for C and H and cc-pVTZ-DK3[56] for La. The DFT calculations were performed with Gaussian 09 software package,[57] whereas the CCSD(T) calculations were carried out with MOLPRO 2010.1.[58]

To compare with the experimental MATI spectra, multidimensional Franck-Condon (FC) factors were calculated from the equilibrium geometries, harmonic vibrational frequencies, and normal coordinates of the neutral and ionized complexes.[59] In these calculations, the recursion relations from the work of Doktorov *et al.*[60] were employed, and the Duschinsky effect[61] was considered to account for a possible axis rotation from the neutral complex to the cation. Spectral simulations were obtained using the experimental line width and Lorentzian line shape. Transitions from excited vibrational levels of the neutral complex were considered by assuming thermal excitation at specific temperatures.

III. RESULTS AND DISCUSSION

A. TOF mass spectra and La-hydrocarbon species

Figure 1 displays the TOF mass spectra of the La reactions with 1-butene, 2-butene, and isobutene recorded with 240-250 nm photoionization. The mass spectra from all the butene reactions are essentially the same and show a predominant product $La(C_4H_6)$ and several other metal-hydrocarbon species. $La(C_4H_6)$ is formed by the loss of H_2 from C_4H_8. $La(C_8H_{14})$,

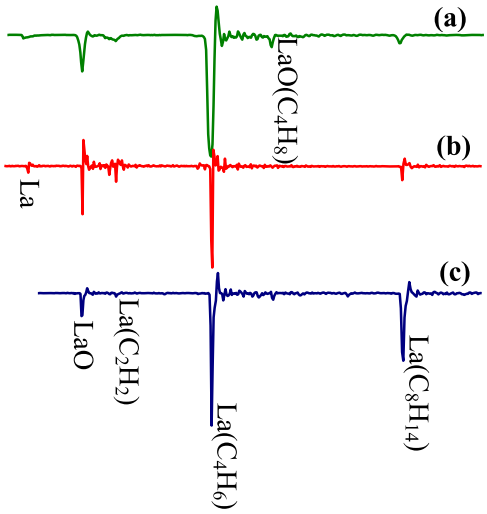

FIG. 1. TOF Mass spectra of La+1-butene (a), La+2-butene (b), and La+isobutene reactions recorded with 240-250 nm photoionization.

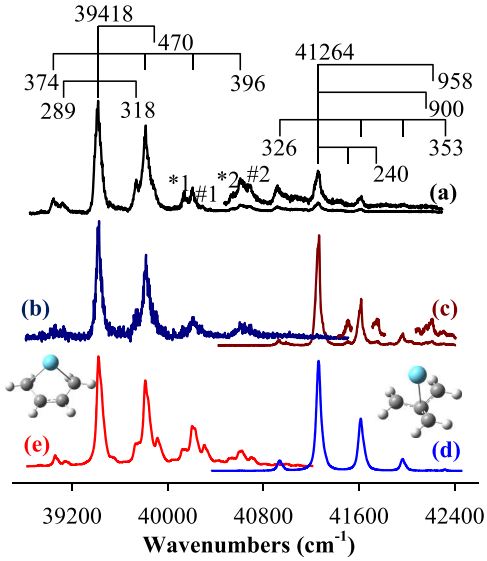

FIG. 2. MATI spectra of $La(C_4H_6)$ produced from La reactions with 1-butene [(a), black], 2-butene [(b), dark blue], and isobutene [(c), dark red] and simulations of the $^1A_1 \leftarrow {}^2A_1$ transition of $La[C(CH_2)_3]$ (C_{3v}) (Iso A) [(d), blue] and the $^1A' \leftarrow {}^2A'$ transition of $La(CH_2CHCHCH_2)$ (C_s) (Iso B) [(e), red] at 300 K.

which is a minor species in the 1- and 2-butene reactions but becomes more significant in the isobutene reaction, is formed by a secondary reaction, possibly $La(C_4H_6)+C_4H_8$. Two other minor species are $La(C_2H_2)$ and $LaO(C_4H_8)$, with the smaller species being formed by the C—C cleavage and the larger one by the addition of LaO with a butene molecule. The observation of the adduct $LaO(C_4H_8)$ suggests that LaO is less reactive than La. LaO could be formed by La reactions with oxygen that is present in the carrier gas as an impurity or by laser vaporization of La oxide impurity in the La rod.[26–28,30–33] The observation of the predominating H_2 loss is similar to previous studies on butene reactions with other metal atoms or ions.[34–48]

B. MATI spectra and isomers of $La(C_4H_6)$

MATI spectra of $La(C_4H_6)$ formed by the La reactions with 1-butene, 2-butene, and isobutene are different as shown in Fig. 2. The spectrum of $La(C_4H_6)$ from the La+1-butene reaction [Fig. 2(a)] displays two band systems, with the stronger band system originating at 39 418 (5) cm^{-1} and the weaker one originating at 41 264 (5) cm^{-1}. The 39 418 cm^{-1} band system consists of a 396 cm^{-1} progression with up to three vibrational quanta, two bands at 318 and 470 cm^{-1}, and several other weaker bands marked with "*1, *2, #1, and #2" at the higher energy side of the origin band. The "*1 and *2" bands are the combination bands of the 318 cm^{-1} transition with the first and second quanta of the 396 cm^{-1} progression, whereas the "#1 and #2" bands are the combination bands of the 470 cm^{-1} transition with the first and second quanta of the 396 cm^{-1} progression, respectively. At the lower energy side, the 39 418 cm^{-1} band system shows two weak bands at 289 and 374 cm^{-1}, which are due to transitions from vibrationally excited levels of the neutral species. The 41 264 cm^{-1} band system is much weaker but clearly displays a 353 cm^{-1} transition at the higher energy side and a 326 cm^{-1} transition at the lower energy side of the origin band. The spectrum of $La(C_4H_6)$ formed by the La+2-butene reaction [Fig. 2(b)] is essentially the same as the 39 418 cm^{-1} band system of the species formed by La+1-butene, though the signal-to-noise ratio is lower. Because of the weaker signals, some of the weak bands are not as well resolved as those in the spectrum from the La+1-butene reaction. On the other hand, the spectrum of $La(C_4H_6)$ produced by La+isobutene has a much higher signal-to-noise ratio [Fig. 2(c)]. It not only reproduces the three bands of the 41 264 cm^{-1} band system of the species formed by the 1-butene reaction but also shows at the higher energy side of the 41 264 cm^{-1} origin band a 240 cm^{-1} progression with up to two quanta, two more quanta of the 353 cm^{-1} progression, and two additional bands at 900 and 958 cm^{-1}.

Figure 3 displays the structures of the doublet ground states of the three low-energy isomers of $La(C_4H_6)$,[32] along with the structures of the singlet ground states of the butene

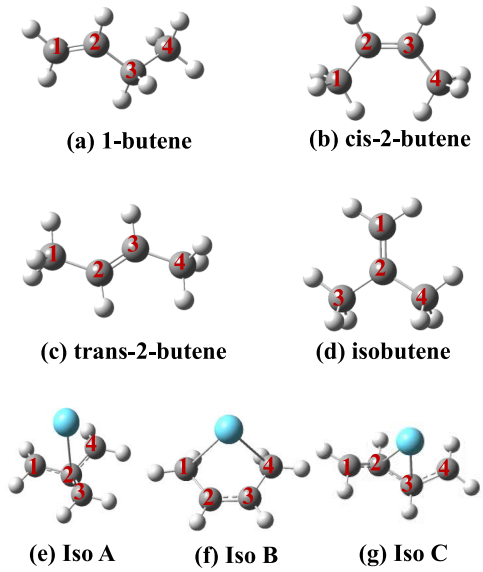

FIG. 3. Structures of the ground states of butene [(a)–(d)] and $La(C_4H_6)$ [(e)–(g)] isomers. Relative energies of these species are listed in Table I.

TABLE I. Point groups, electronic states, and relative energies (E, cm^{-1}) of butene and La(C_4H_6) isomers from B3LYP and CCSD(T)//B3LYP calculations. The energies of 1- and 2-butenes are relative to that of isobutene, and the energies of La($CH_2CHCHCH_2$) (Iso B) and La(*trans*-$CH_2CHCHCH_2$) (Iso C) are relative to that La[$C(CH_2)_3$] (Iso A). All energies include vibrational zero point corrections.

Complex	Point group	State	E_{B3LYP}	$E_{CCSD(T)//B3LYP}$
La[$C(CH_2)_3$] (Iso A)	C_{3v}	$^2A_1$	0	0
	C_s	$^4A''$	16 364	
	C_{3v}	$^1A_1$	41 810	41 008
	C_s	$^3A''$	54 731	
	C_s	$^2A'$	104	1 050
La(*cis*-$CH_2CHCHCH_2$)	C_s	$^4A''$	10 232	
(Iso B)	C_s	$^1A'$	40 268	40 248
	C_s	$^3A'$	49 039	
	C_2	^2A	3 674	4 294
La(*trans*-$CH_2CHCHCH_2$)	C_2	^4B	11 132	
(Iso C)	C_2	^1A	45 468	44 944
	C_1	^3A	50 334	
1-butene	C_1	^1A	1 324	1 386
cis-2-butene	C_{2v}	$^1A_1$	589	849
trans-2-butene	C_{2h}	^1A_g	130	455
Isobutene	C_{2v}	$^1A_1$	0	0

isomers (C_4H_8). Table I lists relative electronic energies including vibrational zero point corrections of various spin states of the La(C_4H_6) isomers predicted by the DFT/B3LYP calculations and the doublet ground states and singlet ion states of those isomers predicted by the CCSD(T) single-point energy calculations. The relative energies of the butenes follow the order of isobutene < 2-butenes < 1-butene. The two conformers of *cis*- and *trans*-2-butene are close in energies, with the *trans* form being slightly more stable. The three isomers of La(C_4H_6) are trimethylenemethanelanthanum {La[$C(CH_2)_3$], Iso A}, 1-lanthanacyclopent-3-ene [La($CH_2CHCHCH_2$), Iso B], and (*trans*-butadiene)lanthanum [La(*trans*-C_4H_6), Iso C]. The most stable isomer is predicted to be Iso A, followed by Iso B and Iso C. For each isomer, the ground state of the neutral species is a doublet state, followed by a quartet state; the lowest energy state of the corresponding ion is a singlet state, followed by a triplet state. At the DFT/B3LYP computational level, the energy differences between the quartet and doublet neutrals are predicted to be 2.03 eV (1 eV = 8065 cm^{-1}) for Iso A, 1.26 eV for Iso B, and 0.92 eV for Iso C. The energy differences between the triple and singlet ions are 1.60 eV for Iso A, 1.09 eV for Iso B, and 0.60 eV for Iso C. The lower spin states in the neutral and ion states are more stable due to the stronger metal-ligand binding, as evidenced by the shorter La—C distances (Table S1 of the supplementary material). Among the neutral doublet states of the three isomers, the $^2A_1$ state of Iso A (C_{3v}) has the lowest energy, the $^2A'$ state of Iso B (C_s) is predicted at ~0.01 eV by B3LYP and 0.13 eV by CCSD(T), and the ^2A state of Iso C (C_2) is at 0.46 and 0.53 eV by the two computational methods.

The 39 418 cm^{-1} band system of La(C_4H_6) from the 1-butene reaction and the spectrum of La(C_4H_6) from the 2-butene reaction are assigned to the $^1A' \leftarrow {}^2A'$ transition of Iso B. The 41 264 cm^{-1} band system of La(C_4H_6) from the 1-butene reaction and the spectrum of La(C_4H_6) from the isobutene reaction are attributed to the $^1A_1 \leftarrow {}^2A_1$ transition of Iso A. These assignments are supported by the agreement between the measurements and computations, as demonstrated in Table II and Fig. 2. Table II summarizes the measured and calculated AIEs and vibrational frequencies. Figure 2 compares the simulated vibronic spectrum of the $^1A' \leftarrow {}^2A'$ transition of Iso B [Fig. 2(e)] to the 39 418 cm^{-1} band system from the 1- and 2-butene reactions [Figs. 2(a) and 2(b)] and the simulated vibronic spectrum of the $^1A_1 \leftarrow {}^2A_1$ transition of Iso A [Fig. 2(d)] to the 41 264 cm^{-1} band system from the 1-butene and isobutene reactions [Figs. 2(a) and 2(c)]. The origin bands in the simulations are aligned with those in the experimental spectra, but the computed vibrational frequencies are unscaled in order to directly compare with the experimental spectrum. For the 39 418 cm^{-1} band system in Figs. 2(a) and 2(b), the 470, 396, and 318 cm^{-1} vibronic bands are assigned to excitations of a symmetric La-ligand stretch coupled with a terminal CH_2 rock (ν_{11}^+, a′), a second symmetric La-ligand stretch mixed with another terminal CH_2 rock (ν_{12}^+, a′), and a symmetric C—H bend of the middle HC=CH group (ν_{13}^+, a′) in the $^1A'$

TABLE II. Adiabatic ionization energies (AIEs, cm^{-1}) and vibrational frequencies (cm^{-1}) of La[$C(CH_2)_3$] (Iso A) and La($CH_2CHCHCH_2$) (Iso B) from MATI spectroscopy and theoretical calculations. ν_n and ν_n^+ are vibrational modes in the neutral and ionic states.

Complex	MATI	B3LYP [CCSD(T)][a]	Mode description
La[$C(CH_2)_3$] (Iso A), C_{3v}, $^1A_1 \leftarrow {}^2A_1$			
AIE	41 264	41 810 (41 008)	
v_3^+, a_1	958	975	$C(CH_2)_3$ deformation
v_4^+, a_1	900	924	CH_2 wag
v_6^+/v_6, a_1	353/326	351/327	Symmetric La-ligand stretch
v_{18}^+, e	240	234	Asymmetric La-ligand stretch
La($CH_2CHCHCH_2$) (Iso B), C_s, $^1A' \leftarrow {}^2A'$			
AIE	39 418	40 164 (39 198)	
v_{11}^+, a′	470	492	Symmetric La-ligand stretch and terminal CH_2 rock
v_{12}^+/v_{12}, a′	396/374	391/359	Symmetric La-ligand stretch and terminal CH_2 rock
v_{13}^+/v_{13}, a′	318/289	309/279	C—H bend of middle C_2H_2 group

[a]The AIE values in parentheses are from CCSD(T) single point energy calculations at the B3LYP geometries.

ion state of Iso B; the 374 and 289 cm^{-1} vibronic bands to the second La-ligand stretch/CH_2 rock (ν_{12}, a′) and C—H bend (ν_{13}, a′) excitations in the $^2A'$ state of the same isomer. The main difference between the two La-ligand stretch/CH_2 rock modes is the opposite directions of the CH_2 rocking motions. For the 41 264 cm^{-1} band system in Figs. 2(a) and 2(c), the $^1A_1 \leftarrow {}^2A_1$ simulation of Iso A reproduces the experimental 353 cm^{-1} vibronic band and the 326 cm^{-1} hot band. The 353/326 cm^{-1} bands are assigned to the symmetric La-ligand stretch excitations (ν_6^+/ν_6, a_1) of the $^1A_1$ ion/$^2A_1$ neutral states. The simulation also reproduces the second and third quanta of the 353 cm^{-1} progression and the weak 900 and 958 cm^{-1} transitions above the origin band in the spectrum of Fig. 2(c). The 900 and 958 cm^{-1} vibronic bands are assigned to the CH_2 wag (ν_4^+, a_1) and $C(CH_2)_3$ deformation (ν_3^+, a_1) of the ion, respectively. However, the weak 240 cm^{-1} progression in Fig. 2(c) is not present in the simulation. This progression was previously attributed to excitations of a degenerate asymmetric La-ligand stretch (ν_{18}^+, e) of $La(C_4H_6)$ formed by the La reaction with propene, and the activity of the degenerate mode could be due to the Herzberg-Teller effect.[32]

Other transitions of Iso A and B can be excluded from the observed MATI spectra. The 0–0 energies of the triplet ← doublet transitions of Iso A and B are predicted to be 54 731 and 49 039 cm^{-1}, respectively, which are much higher than the energies of the experimental origin bands at 39 418 or 41 264 cm^{-1}. Although the 0–0 energies of the triplet ← quartet transitions of the two isomers (38 367 cm^{-1} for Iso A and 38 807 cm^{-1} for Iso B) are not much different from the experimental 39 418 cm^{-1} origin band, the neutral quartet states are excited states at relatively high energies (2.03 eV for Iso A and 1.26 eV for Iso B) so that they are unlikely survived under the supersonic expansion conditions. Similarly, Iso C is not a candidate for the observed spectra because it is in significantly higher energy than the doublet states of either Iso A or B. Furthermore, simulations of the triplet ← doublet or triplet ← quartet transitions do not match the experimental observations.

The $C(CH_2)_3$ fragment in Iso A is a trimethylenemethane diradical, where the π system consists of four π electrons delocalized over four π-type molecular orbitals, two of which are degenerate.[62] In the $^2A_1$ state of Iso A (C_{3v}), $C(CH_2)_3$ has three equal C—C bonds (Table S1 of the supplementary material) and corresponds to the structure of the triplet ground state with two unpaired electrons in the degenerate π orbitals.[62] The $CH_2CHCHCH_2$ moiety in the $^2A'$ state of Iso B (C_s) is a *cis*-butene-1,4-diyl (Table S1) and can also be considered a diradical with an unpaired electron localized on the carbon atom of each CH_2 group. In La binding with these diradicals, the two 5d electrons of La are spin paired in a molecular orbital that is a bonding combination between a La 5d orbital and a π^* unoccupied antibonding orbital of the hydrocarbon fragment. The charge transfer from La to the hydrocarbon leads to a formal oxidation state of +2 for the La atom with largely a La $6s^1$ electron in the highest occupied molecular orbital (HOMO) in the doublet ground states of the two isomers. The removal of the metal-based 6s electron by ionization has a small effect on the geometry of the complex, and thus the MATI spectra of the both isomers display short FC profiles. By contrast, the $C(CH_2)_3$ fragment in the $^4A''$ state of Iso A (C_s) has one longer C—C bond and two shorter ones (Table S1) and corresponds to the structure of a singlet excited state with two π electrons anti-paralleled in the degenerate orbital. The $CH_2CHCHCH_2$ moiety in the $^4A''$ state of Iso B (C_s) is a *cis*-1,3-butadiene neutral molecule rather than a radical. Thus, La does not undergo a two-electron transfer in the $^4A''$ state of either Iso A or Iso B, and the HOMOs of the quartet excited states of the two isomers have a La 5d character.

C. Formation of the two isomers of $La(C_4H_6)$

Previously, we observed $La(C_4H_6)$ formed by La atom reactions with ethylene,[28] propene,[32] and 1,3-butadienes.[30] Iso A was identified from the La+propene reaction, which involves the C—C bond cleavage of propene in the primary reaction and the C—C coupling and dehydrogenation in the secondary reaction. Iso B was detected from the C—C bond coupling of ethylene, the association of 1,3-butadiene, and the C—C cleavage and coupling of propene. The formation of the two isomers of $La(C_4H_6)$ by the La reactions with the butenes is different from those of the above reactions and is discussed below. Figures 4–7 illustrate the DFT/B3LYP computed stationary points for the formation of the two isomers from the H_2 elimination of 1-butene, 2-butene, and isobutene, respectively. These stationary points include reactants, intermediates (IMn), transition states (TSn), and products in their doublet spin states. Energies of the stationary points are reported in Tables S2–S4 of the supplementary material. We consider the concerted H_2 elimination because previous studies have shown that stepwise dehydrogenation paths are less favorable for the metal atom-mediated dehydrogenation of small alkenes and alkynes.[26,28,30–32,63–69]

1. Formation of Iso A and Iso B by La reaction with 1-butene

The formation of Iso B from the La+1-butene reaction consists of La addition to the C=C double bond, La insertion

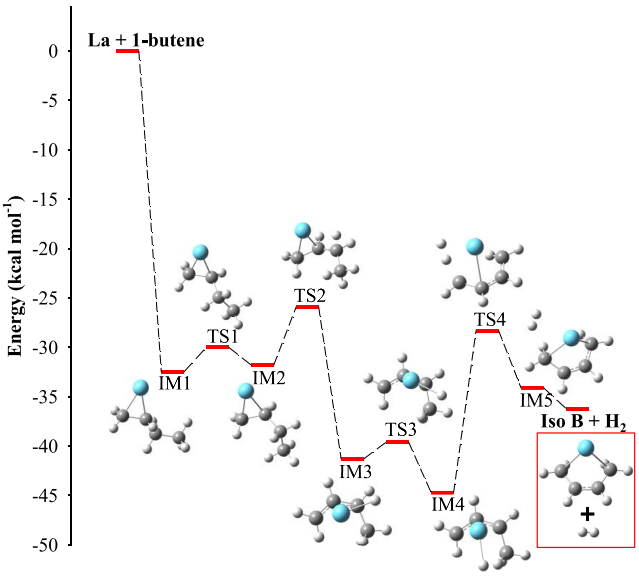

FIG. 4. Reaction pathway and energy profile for the formation of $La(CH_2CHCHCH_2)$ (Iso B) from the La+1-butene reaction at the DFT/B3LYP level, where IMn stands for intermediates and TSn stands for transition states.

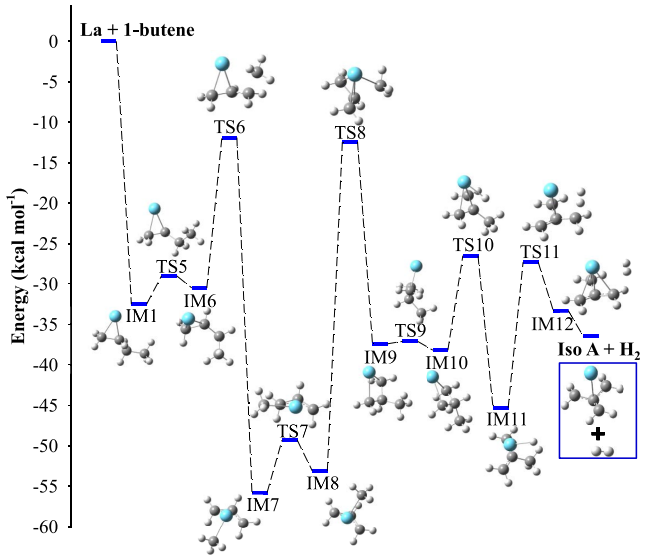

FIG. 5. Reaction pathway and energy profile for the formation of La[C(CH$_2$)$_3$] (Iso A) from the La+1-butene reaction at the DFT/B3LYP level, where IMn stands for intermediates and TSn stands for transition states.

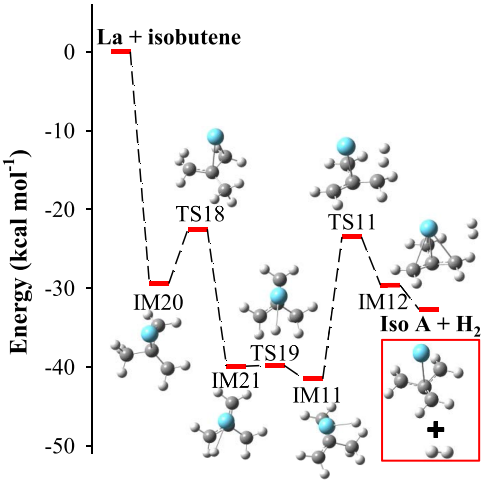

FIG. 7. Reaction pathway and energy profile for the formation of La[C(CH$_2$)$_3$] (Iso A) from the La+isobutene reaction at the DFT/B3LYP level, where IMn stands for intermediates and TSn stands for transition states.

to C(sp^3—H) bonds, and H_2 elimination. Figure 4 and Table S2 of the supplementary material present the stationary points and their energies along the reaction coordinates. The reaction begins with La atom addition to the C=C bond to form a π complex [La(CH$_2$CHCH$_2$CH$_3$), IM1] at 32.5 kcal mol^{-1} below the reactants. Upon the La addition, the C=C double bond of 1-butene is elongated by 0.17 Å (from 1.331 Å to 1.505 Å) due to the cleavage of the π bond between the carbon atoms. The change from the C=C to C—C bond is also evidenced by the bending of the H atoms in the ethenyl group of the ligand. A molecular orbital analysis reveals that the unpaired pπ electron on each of the two ethenyl carbon atoms is paired with a La 5d electron to form a La—σ bond. Thus, the resultant π complex can be considered 2-ethyl-1-lanthanacyclopropane. The exothermic energy from the La addition to 1-butene (32.5 kcal mol^{-1}) is similar to those from La additions to ethylene (32.4 kcal mol^{-1})[28] and propene (29.7 kcal mol^{-1})[31] but significantly lower than those from La additions to propyne (52.3 kcal mol^{-1})[26] and 1- and 2-butynes (52.4 and 51.1 kcal mol^{-1}).[33] The second step (IM1-IM3) is the activation of a C(sp^3)—H bond of the CH_2 group in the β position. The β-carbon is defined as the carbon atom that is connected to the La-bonded α-carbon in the initially formed π complex (IM1). The C(sp^3)—H bond activation involves the rotation of the C$_\alpha$—C$_\beta$ bond via TS1 to convert the trans-conformation of the ligand in IM1 to a cis-conformation in IM2, which is followed by the elongation of a C$_\beta$—H bond via TS2 to form IM3. In IM3, the La—C$_\alpha$ σ bonds are weaker than those in IM2 and a C$_\beta$—H bond is broken; concurrently, the C$_\alpha$—C$_\beta$ bond becomes almost a double bond and a La—H bond is formed. The third step (IM3-IM5) is the activation of a C(sp^3)—H bond of the terminal CH_3 group in the γ position that is next to the β-carbon. This is accomplished by the rotation of the La—H bond in IM3 to form IM4 and the insertion of La into the methyl C(sp^3)—H bond to form IM5. As a result, the C(sp^3)—H bond is cleaved, and additional La—H and La—C(sp^3) bonds are formed. Either of the two La—H bonds in IM5 (2.515 and 2.585 Å) is weaker than the La—H bond in IM4 (2.093 A), and the La-bonded H—H distance (0.768 Å) is close to the equilibrium H—H bond length (0.774 Å) in a free H_2 molecule. The final step is the concerted H_2 elimination from IM5 to form Iso B. The whole process La+1-butene → Iso B is exothermic by 36.2 kcal mol^{-1} and has no overall energy barrier. Along the reaction coordinates, the C(sp^3)—H bond activation is preferred because it is weaker than a C(sp^2)—H bond, C—C or La—H bond rotations have lower barriers (TS1 and TS3) than metal insertions into C—H bonds (TS2 and TS4), and the H_2 elimination (IM5–Iso B) is basically barrierless. Because the energy barriers (TS1-TS4) are considerably lower than the energy of the reactants, all intermediates (IM1-IM5) have tendency to convert to the product (Iso B). This may explain why no intermediates were observed in our experiments even though the two inserted species (IM3 and IM4)

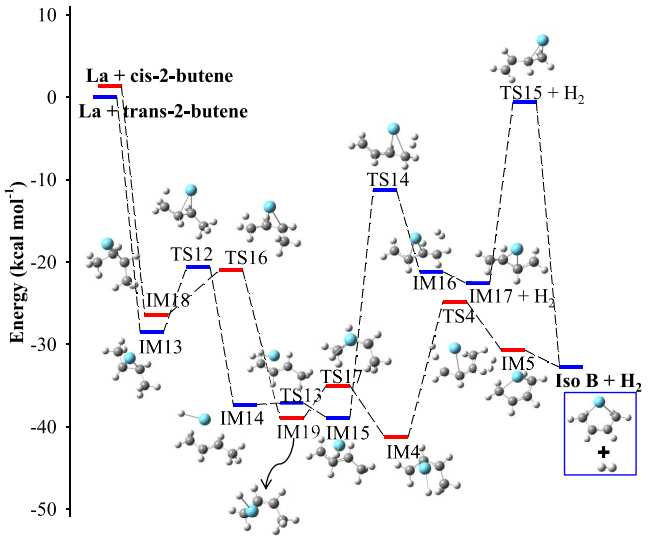

FIG. 6. Reaction pathways and energy profiles for the formation of La(CH$_2$CHCHCH$_2$) (Iso B) from the La+*cis*-2-butene (red) and La+*trans*-2-butene (blue) reactions at the DFT/B3LYP level, where IMn stands for intermediates and TSn stands for transition states.

are more stable than the product. This observation is similar to previous studies of La reactions with other small unsaturated hydrocarbons,[26,28,33] except for propene where a La-inserted species was identified.[31]

The formation of Iso A is more complicated due to the carbon skeleton rearrangement that involves both C—C bond cleavage and coupling prior to H_2 elimination (Fig. 5 and Table S2 of the supplementary material). The first step is the same as that in the formation of Iso B, which is the La addition to form an IM1 π complex. The second step is the C_β—C_γ cleavage (IM1-IM8). This step consists of the C_α—C_β bond rotation to bring the ligand to a cis-conformation to form IM6, the La insertion into the C_β—C_γ bond to form IM7, and the rotation of the La—CH_3 bond to form IM8. IM6 is similar to IM2, except that the C_γ atom in the methyl group is near the La atom. Although both IM7 and IM8 may be considered methyl(η^3-allyl)lanthanum [$(CH_3)La(CH_2CHCH_2)$], the La—CH_3 bonds in the two minima are in almost opposite orientations and the CH_3 group in IM8 is closer to the C_α atom. The third step is the C—C coupling to form 3-methyl-1-lanthanacyclobutane [$La(CH_2CH(CH_3)CH_2)$], where the metallacycle and the methyl group are in a chair (IM9) or a boat conformation (IM10). The final step is the H_2 elimination from two C(sp^3)—H bonds to form Iso A (IM10-Iso A). As in the case of the Iso B formation, the dehydrogenation involves the La insertion into the C_α(sp^3)—H bond to form an inserted species (IM11), a second insertion into a C(sp^3—H) bond of the methyl group to form a dihydrogen complex (IM12), and a concerted H_2 elimination from IM12. The La+1-butene → Iso A reaction is exothermic by 36.5 kcal mol^{-1} and has no overall energy barriers. The C—C cleavage and coupling in the formation of Iso A require more energies (TS6 at 18.6 kcal mol^{-1} and TS8 at 40.7 kcal mol^{-1}) than the C—H bond activation in the Iso B formation (TS2 at 5.9 kcal mol^{-1} and TS4 at 16.4 kcal mol^{-1}). Because of the higher energy barriers, the formation of Iso A is kinetically less favorable than the formation of Iso B. The less favorable kinetics may explain the weaker spectral signal of Iso A even though it is predicted to be slightly more stable than Iso B.

2. Formation of Iso B by La reaction with 2-butene

Because 2-butene used in our experiment is a mixture of the trans and cis conformers, we consider reaction paths for both La+*trans*-2-butene → Iso B (solid blue lines) and La+*cis*-2-butene → Iso B (solid red lines) (Fig. 6 and Table S3 of the supplementary material). Similar to La+1-butene → Iso B, the La-mediated dehydrogenation processes of *trans*- and *cis*-2-butenes include the initial formation of a π complex (IM 13 or IM18), the activation of two C(sp^3)—H bonds in two methyl groups (IM13-IM16 or IM18-IM5), and the concerted H_2 elimination from a dihydrogen complex (IM16-IM17 or IM15-IsoB). Both reactions are thermodynamically favorable with exothermic energies ~32 kcal mol^{-1}. Yet, differences are noted between the *trans*- and *cis*-2-butene reactions. First, after the H_2 elimination the *trans*-2-butene reaction undergoes the isomerization of the $CH_2CHCHCH_2$ fragment from the *trans* form in IM17 to the *cis* form in Iso B and the shift of La binding positions from the middle to the terminal two carbons. IM17, which is the same as Iso C, is about 10 kcal mol^{-1} higher than Iso B. Iso B could also be formed from isomerization followed by dehydrogenation. But this process is expected to be less favorable, as demonstrated by the La-mediated 1,3-butadiene dehydrogenation where H_2 elimination was found to occur before the trans to cis isomerization.[30] Second, the *cis*-2-butene reaction shares two same intermediates (IM4 and IM5) as those of the 1-butene reaction along the coordinates of the Iso B formation. Finally, the energy barriers of the *cis*-2-butene reaction are lower than those of the *trans*-2-butene reaction, suggesting that the former is kinetically more favorable than the latter.

3. Formation of Iso A by La reaction with isobutene

The La-mediated dehydrogenation of isobutene produces only Iso A. The predicted pathway for the formation of Iso A from the isobutene reaction also consists of the formation of a π complex, La insertion into to C(sp^3)—H bonds, and H_2 elimination (Fig. 7 and Table S4 of the supplementary material). These steps are similar to those for the formation of Iso B by the 1-butene or *cis*-2-butene reaction. The reaction begins with the formation of the π complex at −29.4 kcal mol^{-1} (IM20) and proceeds with the La insertion into one of the C(sp^3)—H bonds in a CH_3 group to form an inserted species (IM21). Prior to the second La insertion into a C(sp^3)—H bond in the other CH_3 group, the La—H bond in IM21 rotates to a position where the metal-bonded H atom is in the proximity of the methyl group and to form a new inserted species (IM11). From this point, the reaction proceeds with the same steps as those of the La+1-butene → Iso A reaction (IM11-Iso A). The overall reaction is barrierless and exothermic by 32.7 kcal mol^{-1}.

IV. CONCLUSIONS

We have reported the MATI spectra and formation of $La(C_4H_6)$ formed by the La-mediated dehydrogenation of 1-butene, 2-butene, and isobutene. The spectra of $La(C_4H_6)$ formed in the 1-butene reaction exhibit two band systems, which are assigned to the ionization of the $La[C(CH_2)_3]$ and $La(CH_2CHCHCH_2)$ isomers. The spectra of $La(C_4H_6)$ formed in the 2-butene and isobutene reactions both display a single band system, and the former is attributed to $La(CH_2CHCHCH_2)$ and the later is attributed to $La[C(CH_2)_3]$. The MATI measurements yield AIEs and metal-ligand stretching and ligand-based bending frequencies for the two isomers. The ground state of each isomer is a doublet state with a La-based $6s^1$ electron configuration, and the lowest-energy state of the corresponding ion is a singlet state upon the removal of the La $6s^1$ electron. Because of the non-bonding nature of the La $6s^1$ electron, ionization has a small effect on the geometry of the neutral state. Quantum chemical calculations suggest that formations of the two isomers consist of the La addition to the C=C triple bond, La insertion into C(sp^3)—H bonds, and concerted dehydrogenation. The C—H bond activation takes places after the C—C bond cleavage and coupling in the reaction of La+1-butene to form $La[C(CH_2)_3]$, while it occurs before the trans to cis isomerization in the La+*trans*-2-butene reaction to form $La(CH_2CHCHCH_2)$.

SUPPLEMENTARY MATERIAL

See supplementary material for the geometries of the La(C_4H_6) isomers and the energies of the stationary points along the reaction coordinates for the formation of La[$C(CH_2)_3$] and La($CH_2CHCHCH_2$) formed by La atom reactions with 1-butene, 2-butene, and isobutene.

ACKNOWLEDGMENTS

We are grateful for the financial support from the National Science Foundation Division of Chemistry (Chemical Structure, Dynamics, and Mechanisms, Grant No. CHE-1362102). We also acknowledge additional support from the Kentucky Science and Engineering Foundation.

[1] R. S. Walters, T. D. Jaeger, and M. A. Duncan, J. Phys. Chem. A **106**, 10482 (2002).
[2] R. S. Walters, E. D. Pillai, P. v. R. Schleyer, and M. A. Duncan, J. Am. Chem. Soc. **127**, 17030 (2005).
[3] R. S. Walters, P. V. Schleyer, C. Corminboeuf, and M. A. Duncan, J. Am. Chem. Soc. **127**, 1100 (2005).
[4] A. D. Brathwaite, T. B. Ward, R. S. Walters, and M. A. Duncan, J. Phys. Chem. A **119**, 5658 (2015).
[5] R. B. Metz, Adv. Chem. Phys. **138**, 331 (2008).
[6] G. Altinay, M. Citir, and R. B. Metz, J. Phys. Chem. A **114**, 5104 (2010).
[7] G. Altinay and R. B. Metz, J. Am. Soc. Mass Spectrom. **21**, 750 (2010).
[8] G. Altinay and R. B. Metz, Int. J. Mass spectrom. **297**, 41 (2010).
[9] M. Citir, G. Altinay, G. Austein-Miller, and R. B. Metz, J. Phys. Chem. A **114**, 11322 (2010).
[10] G. Altinay, A. Kocak, J. S. Daluz, and R. B. Metz, J. Chem. Phys. **135**, 084311 (2011).
[11] M. Perera, P. Ganssle, and R. B. Metz, Phys. Chem. Chem. Phys. **13**, 18347 (2011).
[12] M. Perera, R. B. Metz, O. Kostko, and M. Ahmed, Angew. Chem., Int. Ed. **52**, 888 (2013).
[13] A. Kocak, M. A. Ashraf, and R. B. Metz, J. Phys. Chem. A **119**, 9653 (2015).
[14] A. Kocak, Z. Sallese, M. D. Johnston, and R. B. Metz, J. Phys. Chem. A **118**, 3253 (2014).
[15] M. A. Ashraf, C. W. Copeland, A. Kocak, A. R. McEnroe, and R. B. Metz, Phys. Chem. Chem. Phys. **17**, 25700 (2015).
[16] C. W. Copeland, M. A. Ashraf, E. M. Boyle, and R. B. Metz, J. Phys. Chem. A **121**, 2132 (2017).
[17] V. J. F. Lapoutre, B. Redlich, A. F. G. van der Meer, J. Oomens, J. M. Bakker, A. Sweeney, A. Mookherjee, and P. B. Armentrout, J. Phys. Chem. A **117**, 4115 (2013).
[18] O. W. Wheeler, M. Salem, A. Gao, J. M. Bakker, and P. B. Armentrout, J. Phys. Chem. A **120**, 6216 (2016).
[19] S. R. Miller, T. P. Marcy, E. L. Millam, and D. G. Leopold, J. Am. Chem. Soc. **129**, 3482 (2007).
[20] W. Y. Lu, P. D. Kleiber, M. A. Young, and K. H. Yang, J. Chem. Phys. **115**, 5823 (2001).
[21] D. J. Brugh, R. S. Dabell, and M. D. Morse, J. Chem. Phys. **121**, 12379 (2004).
[22] M. A. Garcia and M. D. Morse, J. Phys. Chem. A **117**, 9860 (2013).
[23] D. J. Brugh and M. D. Morse, J. Chem. Phys. **141**, 064304 (2014).
[24] E. L. Johnson and M. D. Morse, Mol. Phys. **113**, 2255 (2015).
[25] M. A. Flory, A. J. Apponi, L. N. Zack, and L. M. Ziurys, J. Am. Chem. Soc. **132**, 17186 (2010).
[26] D. Hewage, M. Roudjane, W. R. Silva, S. Kumari, and D.-S. Yang, J. Phys. Chem. A **119**, 2857 (2015).
[27] D. Hewage, W. R. Silva, W. Cao, and D.-S. Yang, J. Am. Chem. Soc. **138**, 2468 (2016).
[28] S. Kumari, W. Cao, Y. Zhang, M. Roudjane, and D.-S. Yang, J. Phys. Chem. A **120**, 4482 (2016).
[29] Y. Zhang, M. W. Schmidt, S. Kumari, M. S. Gordon, and D.-S. Yang, J. Phys. Chem. A **120**, 6963 (2016).
[30] D. Hewage, W. Cao, J. H. Kim, Y. Wang, Y. Liu, and D.-S. Yang, J. Phys. Chem. A **121**, 1233 (2017).
[31] S. Kumari, W. Cao, D. Hewage, R. Silva, and D.-S. Yang, J. Chem. Phys. **146**, 074305 (2017).
[32] D. Hewage, W. Cao, S. Kumari, R. Silva, T. H. Li, and D.-S. Yang, J. Chem. Phys. **146**, 184304 (2017).
[33] W. Cao, D. Hewage, and D.-S. Yang, J. Chem. Phys. **147**, 064303 (2017).
[34] K. Eller and H. Schwarz, Chem. Rev. **91**, 1121 (1991).
[35] J. C. Weisshaar, Acc. Chem. Res. **26**, 213 (1993).
[36] P. B. Armentrout, L. F. Halle, and J. L. Beauchamp, J. Am. Chem. Soc. **103**, 6624 (1981).
[37] L. S. Sunderlin and P. B. Armentrout, Organometallics **9**, 1248 (1990).
[38] R. L. Hettich and B. S. Freiser, Organometallics **8**, 2447 (1989).
[39] L. M. Lech and B. S. Freiser, Organometallics **7**, 1948 (1988).
[40] P. I. Surya, D. R. A. Ranatunga, and B. S. Freiser, J. Am. Chem. Soc. **119**, 3351 (1997).
[41] H. H. Cornehl, C. Heinemann, D. Schroder, and H. Schwarz, Organometallics **14**, 992 (1995).
[42] V. Baranov, H. Becker, and D. K. Bohme, J. Phys. Chem. A **101**, 5137 (1997).
[43] P. Mourgues, A. Ferhati, T. B. McMahon, and G. Ohanessian, Organometallics **16**, 210 (1997).
[44] W. S. Taylor, A. S. Campbell, D. F. Barnas, L. M. Babcock, and C. B. Linder, J. Chem. Phys. A **101**, 2654 (1997).
[45] J. Marcalo, M. Santos, A. P. de Matos, J. K. Gibson, and R. G. Haire, J. Phys. Chem. A **112**, 12647 (2008).
[46] D. Ritter, J. J. Carroll, and J. C. Weisshaar, J. Phys. Chem. **96**, 10636 (1992).
[47] J. J. Carroll, K. L. Haug, and J. C. Weisshaar, J. Am. Chem. Soc. **115**, 6962 (1993).
[48] J. J. Carroll, K. L. Haug, J. C. Weisshaar, M. R. A. Blomberg, P. E. M. Siegbahn, and M. Svensson, J. Phys. Chem. **99**, 13955 (1995).
[49] J. J. Schroden, C. C. Wang, and H. F. Davis, J. Phys. Chem. A **107**, 9295 (2003).
[50] B. R. Sohnlein, S. G. Li, J. F. Fuller, and D.-S. Yang, J. Chem. Phys. **123**, 014318 (2005).
[51] C. E. Moore, *Atomic Energy Levels* (National Bureau of Standards, Washington, DC, 1971).
[52] M. A. Duncan, T. G. Dietz, and R. E. Smalley, J. Chem. Phys. **75**, 2118 (1981).
[53] D.-S. Yang, J. Phys. Chem. Lett. **2**, 25 (2011).
[54] T. H. Dunning, Jr., J. Chem. Phys. **90**, 1007 (1989).
[55] W. A. de Jong, R. J. Harrison, and D. A. Dixon, J. Chem. Phys. **114**, 48 (2001).
[56] Q. Lu and K. A. Peterson, J. Chem. Phys. **145**, 054111 (2016).
[57] M. J. Frish, G. W. Trucks, H. B. Schlegel, G. E. Scuseria, M. A. Robb, J. R. Cheeseman, G. Scalmani, V. Barone, B. Mennucci, G. A. Petersson, H. Nakatsuji, M. Caricato, X. Li, H. P. Hratchian, A. F. Izmaylov, J. Bloino, and G. Zheng, GAUSSIAN 09, Revision A.01, Gaussian, Inc., Wallingford, CT, 2009.
[58] H.-J. Werner, P. J. Knowles, G. Knizia, F. R. Manby, M. Schutz, P. Celani, T. Korona, R. Lindh, A. Mitrushenkov, G. Rauhut, K. R. Shamasundar, T. B. Adler, R. D. Amos, A. Bernhardsson, A. Berning, D. L. Cooper, M. J. O. Deegan, A. J. Dobbyn, F. Eckert, E. Goll, C. Hampel, A. Hesselmann, G. Hetzer, T. Hre-nar, G. Jansen, C. Koppl, Y. Liu, A. W. Lloyd, R. A. Mata, A. J. May, S. J. McNicholas, W. Meyer, M. E. Mura, A. Nicklass, D. P. O'Neill, P. Palmieri, K. Pfluger, R. Pitzer, M. Reiher, T. Shiozaki, H. Stoll, A. J. Stone, R. Tarroni, T. Thorsteinsson, M. Wang, and A. Wolf, MOLPRO version 2010.1, a package of *ab initio* programs, 2010, see http://www.molpro.net.
[59] S. Li, "Threshold photoionization and ZEKE photoelectron spectroscopy of metal complexes," Ph.D. thesis, University of Kentucky, 2004.
[60] E. V. Doktorov, I. A. Malkin, and V. I. Man'ko, J. Mol. Spectrosc. **64**, 302 (1977).
[61] F. Duschinsky, Acta Physicochim. **7**, 551 (1937).
[62] L. V. Slipchenko and A. I. Krylov, J. Chem. Phys. **118**, 6874 (2003).
[63] Y. Wen, M. Porembski, T. A. Ferrett, and J. C. Weisshaar, J. Phys. Chem. A **102**, 8362 (1998).
[64] M. Porembski and J. C. Weisshaar, J. Phys. Chem. A **105**, 6655 (2001).
[65] R. Z. Hinrichs, J. J. Schroden, and H. F. Davis, J. Phys. Chem. A **107**, 9284 (2003).
[66] T. H. Li and X. G. Xie, J. Phys. Org. Chem. **23**, 768 (2010).
[67] R. Z. Hinrichs, J. J. Schroden, and H. F. Davis, J. Phys. Chem. A **112**, 3010 (2008).
[68] T. H. Li, C. M. Wang, S. W. Yu, X. Y. Liu, H. Fu, and X. G. Xie, J. Mol. Struct.: THEOCHEM **915**, 105 (2009).
[69] P.-P. Ma, Y.-C. Wang, W.-X. Wang, Z.-P. Deng, G.-P. Niu, X.-L. Wang, S. Li, and Y.-W. Zhang, Comput. Theor. Chem. **1085**, 23 (2016).